



# Microwave-assisted synthesis, biological assessment, and molecular modeling of aza-heterocycles: Potential inhibitory capacity of cholinergic enzymes to Alzheimer's disease



Efraín Polo<sup>a</sup>, Luis Prent-Peñaloza<sup>i</sup>, Yeray A. Rodríguez Núñez<sup>c</sup>, Lady Valdés-Salas<sup>b</sup>, Jorge Trilleras<sup>d</sup>, Juan Ramos<sup>e</sup>, José A. Henao<sup>f</sup>, Antonio Galdámez<sup>g</sup>, Alejandro Morales-Bayuelo<sup>h</sup>, Margarita Gutiérrez<sup>i,\*</sup>

<sup>a</sup> Doctorado en Ciencias Mención I+D de Productos Bioactivos, Instituto de Química de Recursos Naturales, Laboratorio de Síntesis Orgánica, Universidad de Talca, Casilla 747, Talca 3460000, Chile

<sup>b</sup> Facultad de Ciencias de la Salud, Escuela de Tecnología Médica, Universidad de Talca, Casilla 747, Talca 3460000, Chile

<sup>c</sup> Departamento de Ciencias Químicas, Facultad de Ciencias Exactas, Universidad Andrés Bello, Quillota 980, Viña del Mar, Chile

<sup>d</sup> Grupo de Investigación en Compuestos Heterocíclicos, Programa de Química, Facultad de Ciencias Básicas, Universidad del Atlántico, Puerto Colombia, Atlántico – Colombia

<sup>e</sup> Instituto de Química Rosario (IQUIR, CONICET-UNR), Suipacha 531, Rosario (S2002LRK), Argentina

<sup>f</sup> Grupo de Investigación en Química Estructural (GIQUE), Escuela de Química, Facultad de Ciencias, Universidad Industrial de Santander, A.A. 678, Carrera 27, Calle 9 Ciudadela Universitaria, Bucaramanga, Colombia

<sup>g</sup> Departamento de Química, Facultad de Ciencias, Universidad de Chile, Chile

<sup>h</sup> Centro de Investigación de Procesos del Tecnológico Comfenalco (CIPTec), programa de Ingeniería Industrial, Fundación Universitaria Tecnológico Comfenalco – Cartagena, Cr 44 D N 30A, 91, Cartagena-Bolívar, Colombia

<sup>i</sup> Laboratorio Síntesis Orgánica y Actividad Biológica (LSO-Act-Bio), Instituto de Química de Recursos Naturales, Universidad de Talca, Casilla 747, Talca 3460000, Chile

## ARTICLE INFO

### Article history:

Received 5 August 2020

Revised 17 September 2020

Accepted 18 September 2020

Available online 20 September 2020

### Keywords:

Pyrazole

Tetrahydroindazole

Crystal structure

Alzheimer Disease

Cholinergic enzymes

Molecular docking

## ABSTRACT

A highly regioselective solvent-free microwave-assisted synthesis of pyrazoles and tetrahydroindazoles based on the condensation of 1,3-diketones with arylhydrazines is described. Compounds were evaluated as cholinesterase inhibitors in order to identify an alternative treatment for Alzheimer's disease. All compounds displayed moderated acetylcholinesterase inhibitory activity and most of the compounds displayed remarkable butyrylcholinesterase inhibitory activity and selectivity. The compounds 3y and 3i with IC<sub>50</sub> of 1.65 and 3.59 μM, respectively, were the most active and selective compounds as butyrylcholinesterase inhibitors. Likewise, the compounds were tested as antioxidants agents, results showed that they have the ability to trap free-radicals. Molecular Docking studies showed a key π-π stacking interaction of most of the compounds with residue Trp82 within of butyrylcholinesterase active site. Molecular quantum similarity field, global and local reactivity descriptors, and the Fukui functions were calculated in the Density Functional Theory framework to analyze the reactivity patterns along with the molecular set.

© 2020 Published by Elsevier B.V.

## 1. Introduction

Alzheimer's disease (AD) is the leading cause of dementia in the elderly. Pathologically, it is characterized by the presence of senile plaques and neurofibrillary tangles (NFTs), which are formed due to the accumulation of β-amyloid peptide (Aβ) and hyperphosphorylated (p-tau) tau protein, respectively.

The number of neurons is reduced and synapses are missed contributing to cholinergic deficits. The pharmacological treatment for AD mainly involves the use of cholinesterase inhibitors (galantamine, donepezil, and rivastigmine) in the mild to moderate phases and glutamatergic antagonists of N-methyl-D-aspartate (NMDA) receptors (memantine) in the moderate to severe phases of the disease. The use of acetylcholinesterase's inhibitors do not stop the progression of the disease but they generate improvements in the clinical features of patients with AD, especially in the cognitive sphere.

\* Corresponding author. Laboratorio Síntesis Orgánica y Actividad Biológica, Instituto de Química de Recursos Naturales, Universidad de Talca, Casilla 747, Talca 3460000, Chile

E-mail address: [mgutierrez@utalca.cl](mailto:mgutierrez@utalca.cl) (M. Gutiérrez).

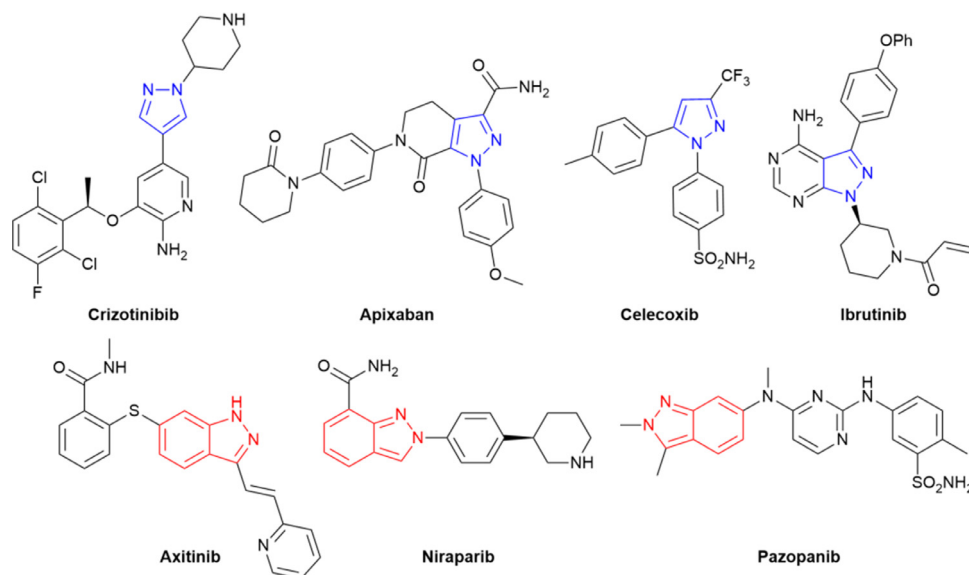


Fig. 1. Examples of biologically active pyrazoles and tetrahydroindazoles.

Acetylcholinesterase (AChE) and butyrylcholinesterase (BuChE) inactivates the neurotransmitter acetylcholine (ACh). Selective inhibitors of BuChE have shown to increase acetylcholine levels in the brain and improve cognition in rodents, as well as lack the classic side effects of AChE inhibitors [1]. Bizarro *et al.* demonstrated that BuChE acts as a modulator of fibrillation of beta-amyloid peptide. They suggest that BuChE could facilitate the formation of a senile plaque of AD. In this way, the inhibition of this enzyme in Alzheimer's treatment can increase the availability of ACh in the synapse as well as reducing the number of senile plaques formed [2].

Moreover, the ring of pyrazoles or indazoles are present in some drugs such as Celecoxib (Celebrex®) demonstrating anti-inflammatory effect and inhibits COX-2 [3]; Apixaban (Eliquis®) is an oral anticoagulant with highly selective inhibition of factor Xa [4]; Ibrutinib (Imbruvica®) for the treatment of mantle cell lymphoma (MCL) and for chronic lymphocytic leukemia (CLL) [5]; Crizotinib (Xalkori®) was approved for the treatment of advanced or metastatic non-small cell lung cancer (NSCLC) that is caused by the echinoderm microtubule-associated proteinlike 4 (EML4) mutation of ALK [6]. Axitinib (Inlyta®) for the treatment of advanced renal cell carcinoma (RCC), specifically after the failure of other systemic treatments [7]; Niraparib (Zejula™) used for Ovarian Cancer (Fig. 1).

Turkan *et al.* synthesized pyrazole derivatives and assayed against AChE and another enzyme. Their results showed that pyrazoles had a moderated inhibitory effect against AChE [8]. In the same way, Kumar *et al.* prepared a set of pyrazoles and tested against AChE, they report that pyrazoles derivative had a good inhibition effect [9].

On the other hand, Khan *et al.* synthesized a tetrahydroindazoles derivatives and tested their potential inhibitory capacity against cholinergic enzymes as well as its potential antioxidant effect. They concluded that the synthesized compounds have a considerable enzymatic inhibitory effect as well as antioxidant effect [10]. The potential pharmacological applications of pyrazole derivatives, maintain interest in the design of synthetic protocols that allow reaching a series of structures, preferably under mild, reproducible conditions and low environmental impact [11,12]. In this study, we synthesized a set of pyrazoles and tetrahydroindazoles derivative (3a-ac) in mild conditions and tested their potential inhibitory capacity against AChE, BuChE, and their antioxidant capac-

ity. At the same time, molecular docking and molecular quantum similarity calculations were made to understand interactions mode in AChE and BuChE-compounds complex.

## 2. Experimental

### 2.1. Materials and methods

The experiments were performed in a Discover microwave apparatus (CEM Corporation, Matthews, NC, USA); All the products were characterized by spectral data (IR, MS,  $^1\text{H-NMR}$ ,  $^{13}\text{C-NMR}$ ).  $^1\text{H}$  and  $^{13}\text{C}$  NMR spectra (400 MHz for proton and 100 MHz for carbon) were recorded on an AM-400 spectrometer (Bruker, Rheinstetten, Germany), using  $\text{CDCl}_3$ ,  $\text{DMSO-d}_6$ , and  $\text{CD}_3\text{OD}$  as solvents. Tetramethylsilane (TMS) was used as an internal standard. IR spectra (KBr pellets,  $500\text{--}4000\text{ cm}^{-1}$ ) were recorded on a NEXUS 670 FT-IR spectrophotometer (Thermo Nicolet, Madison, WI, USA). High-resolution mass spectrometry ESI-MS and ESI-MS/MS analyses were conducted in a high-resolution hybrid quadrupole (Q) and orthogonal time-of-flight (TOF) mass spectrometer (Waters/Micromass Q-TOF micro, Manchester, UK) with a constant nebulizer temperature of  $100^\circ\text{C}$ . Melting points (uncorrected) were measured on an Electrothermal IA9100 melting point apparatus (Stone, Staffs, UK). Reaction progress was monitored by means of TLC using silica gel 60 (Merck, Darmstadt, Germany). All reagents were purchased from either Merck or Sigma Aldrich (St. Louis, MO, USA) and used without further purification. Final purification of all products for analysis was carried out by recrystallization.

### 2.2. General procedure synthesis

A mixture of 1,3-dione (1 mmol) 1a – d and hydrazine derivative (1 mmol) 2a – i was subjected to solvent free microwave irradiation ( $150^\circ\text{C}$ , 10 min). Azoles 3a – ac were readily purified by column chromatography using 5–20% EtOAc–hexanes as eluent. The synthesized compounds with their physical data are listed below.

3a. 3-methyl-2-phenyl-4,5,6,7-tetrahydro-2H-indazole [13–15]. Yield 90 %; brown Oil;  $^1\text{H NMR}$  (400 MHz,  $\text{CDCl}_3$ ):  $\delta_{\text{H}} = 1.57\text{--}1.65$  (m, 4H), 2.01 (s, 3H), 2.28 (t,  $J = 6.0$  Hz, 2H), 2.54 (t,  $J = 6.0$  Hz, 2H), 7.08–7.12 (m, 1H), 7.19–7.24 (m, 4H);  $^{13}\text{C NMR}$  (100 MHz,

CDCl<sub>3</sub>):  $\delta_C = 10.8$  (CH<sub>3</sub>), 20.5 (CH<sub>2</sub>), 23.4 (2 x CH<sub>2</sub>), 23.5 (CH<sub>2</sub>), 115.4 (C), 124.4 (2 x CH), 126.8 (CH), 128.9 (2 x CH), 134.5 (C), 140.2 (C), 149.7 (C); HRMS (ESI, m/z): Calcd for C<sub>14</sub>H<sub>18</sub>N<sub>2</sub> [M+H]<sup>+</sup> 213.1392 found 213.1394.

### 3b. 3-methyl-4,5,6,7-tetrahydro-2H-indazole.

Yield 90 %; brown Oil; IR (KBr, cm<sup>-1</sup>): 3152, 2932, 2842, 1702, 1595, 1436, 1323, 1132, 1074, 993, 929, 842, 753, 619; <sup>1</sup>H NMR (400 MHz, CDCl<sub>3</sub>):  $\delta_H = 1.64$  (m, 4H), 2.08 (s, 3H), 2.18 (m, 1H), 2.29 (t, *J* = 5.6 Hz, 2H), 2.53 (t, *J* = 5.6 Hz, 2H), 9.75 (bs, 1H); <sup>13</sup>C NMR (100 MHz, CDCl<sub>3</sub>):  $\delta_C = 10.4$  (CH<sub>3</sub>), 20.0 (CH<sub>2</sub>), 22.3 (CH<sub>2</sub>), 23.0 (CH<sub>2</sub>), 23.4 (CH<sub>2</sub>), 112.8 (C), 140.9 (C), 144.2 (C); HRMS (ESI, m/z): Calcd for C<sub>14</sub>H<sub>18</sub>N<sub>2</sub> [M]<sup>+</sup> 136.1000 found 136.1067.

### 3c. 4-(3-methyl-4,5,6,7-tetrahydro-2H-indazol-2-yl)benzotrile

[15,16].

Yield 37%; white solid; mp 178 -180°C; <sup>1</sup>H NMR (400 MHz, CD<sub>3</sub>OD):  $\delta_H = 1.74$  (bs, 4H), 2.22 (s, 3H), 2.43 (s, 2H), 2.60 (s, 2H), 7.58 (d, *J* = 8.0 Hz, 2H), 7.77 (d, *J* = 8.0 Hz, 2H); <sup>13</sup>C NMR (100 MHz, CD<sub>3</sub>OD):  $\delta_C = 11.2$  (CH<sub>3</sub>), 21.1 (CH<sub>2</sub>), 23.8 (CH<sub>2</sub>), 24.1 (2 x CH<sub>2</sub>), 110.9 (C), 118.1 (C), 123.2 (C), 125.2 (2 x CH), 134.3 (2 x CH), 136.8 (C), 144.5 (C), 152.4 (C).

### 3d. 2-(4-bromophenyl)-3-methyl-4,5,6,7-tetrahydro-2H-indazole

[15,16].

Yield 90%; brown solid; mp 150-152°C; <sup>1</sup>H NMR (400 MHz, CDCl<sub>3</sub>):  $\delta_H = 1.69$  (bs, 4H), 2.12 (s, 3H), 2.37 (s, 2H), 2.62 (s, 2H), 7.23 (s, 2H), 7.43 (s, 2H); <sup>13</sup>C NMR (100 MHz, CDCl<sub>3</sub>):  $\delta_C = 10.9$  (CH<sub>3</sub>), 20.5 (CH<sub>2</sub>), 23.3 (CH<sub>2</sub>), 23.5 (2 x CH<sub>2</sub>), 115.9 (C), 125.7 (2 x CH), 132.1 (2 x CH), 134.5 (C), 138.6 (C), 139.3 (C), 150.3 (C); HRMS (ESI, m/z): Calcd for C<sub>14</sub>H<sub>16</sub>BrN<sub>2</sub> [M+H]<sup>+</sup> 291.0497 found 291.0483.

### 3e. 4-(3-methyl-4,5,6,7-tetrahydro-2H-indazol-2-yl)benzoic acid

[15].

Yield 40%; Orange crystal; mp 150-152°C; <sup>1</sup>H NMR (400 MHz, DMSO-*d*<sub>6</sub>):  $\delta_H = 1.74$ -1.68 (m, 4H), 2.26 (s, 3H), 2.42 (t, *J* = 5.8 Hz, 2H), 2.57 (t, *J* = 5.8 Hz, 2H), 7.63 (d, *J* = 8.9 Hz, 1H), 8.02 (d, *J* = 8.9 Hz, 1H), 12.98 (s, 1H); <sup>13</sup>C NMR (400 MHz, DMSO-*d*<sub>6</sub>):  $\delta_C = 10.9$  (CH<sub>3</sub>), 19.8 (CH<sub>2</sub>), 22.7 (CH<sub>2</sub>), 22.8 (CH<sub>2</sub>), 22.9 (CH<sub>2</sub>), 116.0 (C), 122.7 (2 x CH), 128.2 (C), 130.2 (2 x CH), 134.5 (C), 143.3 (C), 149.7 (C), 166.7 (C); HRMS (ESI, m/z): Calcd for C<sub>15</sub>H<sub>16</sub>N<sub>2</sub>O<sub>2</sub> [M]<sup>+</sup> 256.1212 found 256.9036

### 3f. 2-(4-chlorophenyl)-3-methyl-4,5,6,7-tetrahydro-2H-indazole

[16,17].

Yield 40%; <sup>1</sup>H NMR (400 MHz, CDCl<sub>3</sub>):  $\delta_H = 1.62$  - 1.69 (m, 4H), 2.06 (s, 3H), 2.32 (t, *J* = 6.0 Hz, 2H), 2.56 (t, *J* = 6.0 Hz, 2H), 7.22- 7.24 (m, 3H), 7.26- 7.28 (m, 1H); <sup>13</sup>C NMR (100 MHz, CDCl<sub>3</sub>):  $\delta_C = 10.8$  (CH<sub>3</sub>), 20.4 (CH<sub>2</sub>), 23.3 (CH<sub>2</sub>), 23.4 (2 x CH<sub>2</sub>), 115.9 (C), 125.5 (2 x CH), 129.1 (2 x CH), 132.4 (C), 134.6 (C), 138.7 (C), 150.2 (C); HRMS (ESI, m/z): Calcd for C<sub>14</sub>H<sub>16</sub>ClN<sub>2</sub> [M+H]<sup>+</sup> 247.1002 found 247.1000.

### 3g. 2-(4-fluorophenyl)-3-methyl-4,5,6,7-tetrahydro-2H-indazole

[15,16].

Yield 40%; <sup>1</sup>H NMR (400 MHz, CDCl<sub>3</sub>):  $\delta_H = 1.89$  - 1.91 (m, 4H), 2.31 (s, 3H), 2.59 (t, *J* = 6.0 Hz, 2H), 2.84 (t, *J* = 6.0 Hz, 2H), 7.22 (d, *J* = 8.0 Hz, 2H), 7.49- 7.52 (m, 2H); <sup>13</sup>C NMR (100 MHz, CDCl<sub>3</sub>):  $\delta_C = 10.8$  (CH<sub>3</sub>), 20.4 (CH<sub>2</sub>), 23.3 (CH<sub>2</sub>), 23.4 (2 x CH<sub>2</sub>), 115.9 (C), 125.5 (2 x CH), 129.1 (2 x CH), 132.4 (C), 134.6 (C), 138.7 (C), 150.2 (C); <sup>13</sup>C NMR (100 MHz, CDCl<sub>3</sub>):  $\delta_C = 10.6$  (CH<sub>3</sub>), 20.4 (CH<sub>2</sub>), 23.3 (2 x CH<sub>2</sub>), 23.4 (CH<sub>2</sub>), 115.6 (CH), 116.2 (C), 126.2 (2 x CH), 134.5 (C), 138.6 (C), 149.8 (C), 160.1 (C-*F*), 162.5 (C-*F*); HRMS (ESI, m/z): Calcd for C<sub>14</sub>H<sub>16</sub>FN<sub>2</sub> [M+H]<sup>+</sup> 231.1298 found 231.1305.

### 3h. 2-(2,4-difluorophenyl)-3-methyl-4,5,6,7-tetrahydro-2H-indazole [16,18].

Yield 40%; <sup>1</sup>H NMR (400 MHz, CDCl<sub>3</sub>):  $\delta_H = 1.57$  - 1.64 (m, 4H), 1.87 (s, 3H), 2.28 (t, *J* = 6.0 Hz, 2H), 2.51 (t, *J* = 6.0 Hz, 2H), 6.72 - 6.78 (m, 2H), 7.19- 7.25 (m, 1H); <sup>13</sup>C NMR (100 MHz, CDCl<sub>3</sub>):  $\delta_C = 11.6$  (CH<sub>3</sub>), 20.3 (CH<sub>2</sub>), 23.3 (2 x CH<sub>2</sub>), 23.4 (CH<sub>2</sub>), 104.6 (CH), *J*<sub>C-F</sub> = 25 Hz), 111.6 (CH, *J*<sub>C-F</sub> = 22 Hz), 124.2 (C, *J*<sub>C-F</sub> = 12 Hz), 129.5 (CH, *J*<sub>C-F</sub> = 10 Hz), 130.1 (C, *J*<sub>C-F</sub> = 12 Hz), 150.6 (C), 155.2 (C,

*J*<sub>C-F</sub> = 12 Hz), 158.1 (C, *J*<sub>C-F</sub> = 12 Hz), 160.9 (C, *J*<sub>C-F</sub> = 11 Hz), 163.4 (C, *J*<sub>C-F</sub> = 11 Hz); HRMS (ESI, m/z): Calcd for C<sub>14</sub>H<sub>15</sub>F<sub>2</sub>N<sub>2</sub> [M+H]<sup>+</sup> 249.1203 found 249.1214.

### 3i. 3-methyl-2-(naphthalen-1-yl)-4,5,6,7-tetrahydro-2H-indazole.

Yield 40%; mp, IR (KBr, cm<sup>-1</sup>): <sup>1</sup>H NMR (400 MHz, CDCl<sub>3</sub>):  $\delta_H = 1.78$ -1.91 (m, 4H), 2.01 (s, 3H), 2.34-2.36 (m, 2H), 2.59 (s, 2H), 7.47-7.56 (m, 5H), 7.93 (d, *J* = 8.0 Hz, 2H); <sup>13</sup>C NMR (100 MHz, CDCl<sub>3</sub>):  $\delta_C = 9.7$  (CH<sub>3</sub>), 20.4 (CH<sub>2</sub>), 21.9 (CH<sub>2</sub>), 23.4 (2 x CH<sub>2</sub>), 113.8 (CH), 114.5 (C), 123.3 (CH), 125.1 (CH), 126.3 (CH), 126.8 (C), 126.9 (CH), 127.8 (CH), 128.8 (CH), 130.7 (C), 136.5 (C), 140.8 (C), 149.5 (C); HRMS (ESI, m/z): Calcd for C<sub>18</sub>H<sub>19</sub>N<sub>2</sub> [M+H]<sup>+</sup> 263.1548 found 263.1546.

### 3j. 3-methyl-2-phenyl-2,4,5,6-tetrahydrocyclopenta[c]pyrazole.

Yield 99%; orange crystal; mp 57-59°C; IR (KBr, cm<sup>-1</sup>): 2929, 1708, 1595, 1514, 1375, 1106, 1022, 891, 753, 692; <sup>1</sup>H NMR (400 MHz, CDCl<sub>3</sub>):  $\delta_H = 2.13$  (s, 3H), 2.42 (m, 4H), 2.79 (m, 2H), 7.03 (t, *J* = 8.0 Hz, 1H), 7.23 (t, *J* = 8.0 Hz, 2H), 7.44 (d, *J* = 8.0 Hz, 2H); <sup>13</sup>C NMR (100 MHz, CDCl<sub>3</sub>):  $\delta_C = 12.7$  (CH<sub>3</sub>), 22.3 (CH<sub>2</sub>), 26.8 (CH<sub>2</sub>), 30.9 (CH<sub>2</sub>), 118.6 (2 x CH), 125.0 (CH), 128.3 (C), 129.1 (2 x CH), 140.4 (C), 143.9 (C), 148.9 (C); HRMS (ESI, m/z): Calcd for C<sub>13</sub>H<sub>14</sub>N<sub>2</sub> [M]<sup>+</sup> 198.1157 found 198.1167.

### 3k. 3-methyl-1,4,5,6-tetrahydrocyclopenta[c]pyrazole [19].

Yield 99%; Brown solid; mp 173-175°C; <sup>1</sup>H NMR (400 MHz, CDCl<sub>3</sub>):  $\delta_H = 2.17$  (s, 3H), 2.37 (m, 2H), 2.49 (m, 2H), 2.64 (m, 2H), 10.63 (bs, 1H).

### 3l. 4-(3-methyl-5,6-dihydrocyclopenta[c]pyrazol-2(4H)yl) benzonitrile [16].

Yield 57%; white solid; mp 168-170°C; <sup>1</sup>H NMR (400 MHz, CDCl<sub>3</sub>):  $\delta_H = 2.20$  (s, 3H), 2.53-2.60 (m, 4H), 2.93-2.97 (m, 2H), 7.59 (d, *J* = 8.0 Hz, 2H), 7.64 (d, *J* = 8.0 Hz, 2H); <sup>13</sup>C NMR (100 MHz, CDCl<sub>3</sub>):  $\delta_C = 12.7$  (CH<sub>3</sub>), 22.1 (CH<sub>2</sub>), 27.3 (CH<sub>2</sub>), 30.8 (CH<sub>2</sub>), 107.6 (C), 117.9 (2 x CH), 118.7 (C), 130.2 (C), 133.4 (2 x CH), 143.4 (C), 145.9 (C), 149.1 (C); HRMS (ESI, m/z): Calcd for C<sub>14</sub>H<sub>14</sub>N<sub>3</sub> [M+H]<sup>+</sup> 224.1188 found 224.1198.

### 3m. 2-(4-bromophenyl)-3-methyl-2,4,5,6-tetrahydrocyclopenta[c]pyrazole.

Yield 66%; yellow crystal; mp 85-87°C; IR (KBr, cm<sup>-1</sup>): 2958, 2856, 1589, 1496, 1375, 1288, 1068, 822; <sup>1</sup>H NMR (400 MHz, CDCl<sub>3</sub>):  $\delta_H = 2.26$  (s, 3H), 2.59 (m, 4H), 2.94 (m, 2H), 7.48 (m, 4H); <sup>13</sup>C NMR (90 MHz, CDCl<sub>3</sub>):  $\delta_C = 12.6$  (CH<sub>3</sub>), 22.2 (CH<sub>2</sub>), 26.9 (CH<sub>2</sub>), 30.9 (CH<sub>2</sub>), 119.8 (2 x CH), 132.1 (2 x CH); HRMS (ESI, m/z): Calcd for C<sub>13</sub>H<sub>14</sub>BrN<sub>2</sub> [M+H]<sup>+</sup> 277.0340 found 277.0349.

### 3n. 4-(3-methyl-5,6-dihydrocyclopenta[c]pyrazol-2(4H)yl)benzoic acid.

Yield 18%; brown solid; IR (KBr, cm<sup>-1</sup>): <sup>1</sup>H NMR (400 MHz, DMSO-*d*<sub>6</sub>):  $\delta_H = 2.12$  (s, 3H), 2.46-2.49 (m, 4H), 2.96 (t, *J* = 6.3 Hz, 2H), 7.64 (d, *J* = 8.0 Hz, 2H), 7.96 (d, *J* = 8.0 Hz, 2H), 12.71 (bs, 1H); <sup>13</sup>C NMR (100 MHz, DMSO-*d*<sub>6</sub>):  $\delta_C = 12.3$  (CH<sub>3</sub>), 21.3 (CH<sub>2</sub>), 26.3 (CH<sub>2</sub>), 30.1 (CH<sub>2</sub>), 116.8 (2xCH), 126.5 (C), 128.7 (C), 130.6 (2xCH), 142.8 (C), 144.0 (C), 148.7 (C), 166.6 (C).

### 3o. 2-(4-chlorophenyl)-3-methyl-2,4,5,6-tetrahydrocyclopenta[c]pyrazole [16].

Yield 41%; brown oil; <sup>1</sup>H NMR (400 MHz, DMSO-*d*<sub>6</sub>):  $\delta_H = 2.20$  (s, 3H), 2.56 (m, 4H), 2.96 (m, 2H), 7.61 (m, 4H); <sup>13</sup>C NMR (100 MHz, DMSO-*d*<sub>6</sub>):  $\delta_C = 12.4$  (CH<sub>3</sub>), 21.7 (CH<sub>2</sub>), 26.2 (CH<sub>2</sub>), 30.5 (CH<sub>2</sub>), 119.6 (2 x CH), 128.4 (C), 129.4 (2 x CH), 138.5 (C), 143.4 (C), 149.0 (C), 160.8 (C).

### 3p. 2-(4-fluorophenyl)-3-methyl-2,4,5,6-tetrahydrocyclopenta[c]pyrazole.

Yield 52%; brown solid; mp 118-120°C; IR (KBr, cm<sup>-1</sup>): 2920, 2851, 1615, 1517, 1375, 1221, 1103, 845, 796, 596; <sup>1</sup>H NMR (400 MHz, CDCl<sub>3</sub>):  $\delta_H = 2.40$  (s, 3H), 2.74 (m, 4H), 3.08 (m, 2H), 7.23 (m, 2H), 7.68 (m, 2H); <sup>13</sup>C NMR (100 MHz, CDCl<sub>3</sub>):  $\delta_C = 12.6$  (CH<sub>3</sub>), 22.3 (CH<sub>2</sub>), 26.6 (CH<sub>2</sub>), 31.0 (CH<sub>2</sub>), 115.7 (CH), 116.0 (CH), 120.3 (2 x CH, *J* = 28), 128.3 (C), 136.8 (C), 143.9 (C), 148.8 (C), 159.0 (C),

161.4 (C); HRMS (ESI, m/z): Calcd for  $C_{13}H_{14}FN_2$  [M+H]<sup>+</sup> 217.1141 found 217.1137.

3q. 2-(2,4-difluorophenyl)-3-methyl-2,4,5,6-tetrahydro cyclopenta[c]pyrazole.

Yield 98%; brown oil; IR (KBr,  $cm^{-1}$ ): 2964, 2862, 1523, 1270, 1110, 963, 837, 736, 605, 596; <sup>1</sup>H NMR (400 MHz,  $CDCl_3$ ):  $\delta_H$  = 2.51 (s, 3H), 2.79-2.89 (m, 4H), 2.98-3.02 (m, 2H), 7.17-7.23 (m, 2H), 7.80-7.86 (m, 1H); <sup>13</sup>C NMR (100 MHz,  $CDCl_3$ ):  $\delta_C$  = 12.6 (CH<sub>3</sub>), 22.7 (CH<sub>2</sub>), 25.2 (CH<sub>2</sub>), 30.8 (CH<sub>2</sub>), 104.7 (CH,  $J_{C-F}$  = 25.0 Hz), 111.7 (CH,  $J_{C-F}$  = 21.5 Hz), 127.2 (CH,  $J_{C-F}$  = 9.5 Hz), 144.8 (C), 151.9 (C), 153.4 (C,  $J_{C-F}$  = 11.0 Hz), 155.9 (C,  $J_{C-F}$  = 13.0 Hz), 159.7 (C,  $J_{C-F}$  = 11.0 Hz), 162.2 (C,  $J_{C-F}$  = 11.0 Hz); HRMS (ESI, m/z): Calcd for  $C_{13}H_{12}F_2N_2$  [M]<sup>+</sup> 234.0969 found 234.0964

3r. 2,3-diphenyl-4,5,6,7-tetrahydro-2H-indazole [20–26].

Yield 79%; red crystal; mp 104–106°C; <sup>1</sup>H NMR (400 MHz,  $CDCl_3$ ):  $\delta_H$  = 1.84 (m, 4H), 2.60 (t,  $J$  = 6.0 Hz, 2H), 2.83 (t,  $J$  = 6.0 Hz, 2H), 7.21 (m, 8H), 7.49 (m, 2H); <sup>13</sup>C NMR (100 MHz,  $CDCl_3$ ):  $\delta_C$  = 21.5 (CH<sub>2</sub>), 23.3 (CH<sub>2</sub>), 23.5 (CH<sub>2</sub>), 23.6 (CH<sub>2</sub>), 116.8 (C), 124.7 (2 x CH), 126.5 (CH), 127.7 (CH), 128.4 (2 x CH), 128.7 (2 x CH), 129.2 (2 x CH), 130.8 (C), 138.4 (C), 140.4 (C), 150.3 (C); HRMS (ESI, m/z): Calcd for  $C_{19}H_{20}N_2$  [M+H]<sup>+</sup> 275.1548 found 275.1547.

3s. 3-phenyl-4,5,6,7-tetrahydro-2H-indazole [20,27–29].

Yield 99%; brown solid; mp 213–215°C; <sup>1</sup>H NMR (400 MHz,  $CDCl_3$ ):  $\delta_H$  = 1.78–1.83 (m, 4H), 2.64 (t,  $J$  = 5.6 Hz, 2H), 2.71 (t,  $J$  = 5.6 Hz, 2H), 7.28 (t,  $J$  = 7.3 Hz, 1H), 7.38 (t,  $J$  = 7.6 Hz, 2H), 7.63 (d,  $J$  = 7.6 Hz, 2H), 10.87 (bs, 1H); HRMS (ESI, m/z): Calcd for  $C_{13}H_{15}N_2$  [M+H]<sup>+</sup> 199.1235 found 199.1218.

3t. 4-(3-phenyl-4,5,6,7-tetrahydro-2H-indazol-2-yl)benzotrile.

Yield 72%; white crystal; mp 130–132°C; IR (KBr,  $cm^{-1}$ ): 3050, 2937, 2842, 2226, 1603, 1514, 1369, 1155, 970, 839, 761, 700, 544; <sup>1</sup>H NMR (400 MHz,  $CDCl_3$ ):  $\delta_H$  = 1.76–1.80 (m, 2H), 1.87–1.91 (m, 2H), 2.56 (t,  $J$  = 6.0 Hz, 2H), 2.80 (t,  $J$  = 6.0 Hz, 2H), 7.18 (m, 2H), 7.31–7.36 (m, 5H), 7.53 (d,  $J$  = 8.0 Hz, 1H), 7.70 (d,  $J$  = 8.0 Hz, 1H); <sup>13</sup>C NMR (100 MHz,  $CDCl_3$ ):  $\delta_C$  = 21.1 (CH<sub>2</sub>), 23.1 (CH<sub>2</sub>), 23.2 (CH<sub>2</sub>), 23.4 (CH<sub>2</sub>), 109.3 (C), 118.4 (C), 118.5 (C), 124.1 (2 x CH), 128.3 (CH), 128.7 (2 x CH), 129.1 (2 x CH), 130.2 (C), 132.7 (2 x CH), 138.6 (C), 143.6 (C), 151.8 (C); HRMS (ESI, m/z): Calcd for  $C_{20}H_{18}N_3$  [M+H]<sup>+</sup> 300.1501 found 300.1520.

3u. 2-(4-bromophenyl)-3-phenyl-4,5,6,7-tetrahydro-2H-indazole.

Yield 92%; brown solid; mp 121–123°C; IR (KBr,  $cm^{-1}$ ): <sup>1</sup>H NMR (400 MHz,  $CDCl_3$ ):  $\delta_H$  = 1.77 (m, 2H), 1.88 (m, 2H), 2.56 (t,  $J$  = 6.0 Hz, 2H), 2.79 (t,  $J$  = 6.0 Hz, 2H), 7.11 (m, 2H), 7.15 (dd,  $J$  = 7.6, 1.8, 2H), 7.30 (m, 2H), 7.36 (m, 2H); <sup>13</sup>C NMR (100 MHz,  $CDCl_3$ ):  $\delta_C$  = 21.4 (CH<sub>2</sub>), 23.2 (CH<sub>2</sub>), 23.4 (CH<sub>2</sub>), 23.5 (CH<sub>2</sub>), 117.3 (C), 119.9 (C), 126.0 (2 x CH), 128.0 (CH), 128.5 (2 x CH), 129.2 (2 x CH), 130.5 (C), 131.8 (2 x CH), 138.4 (C), 139.4 (C), 150.7 (C); HRMS (ESI, m/z): Calcd for  $C_{19}H_{19}BrN_2$  [M+H]<sup>+</sup> 353.0653 found 353.0666.

3v. 2-(4-chlorophenyl)-3-phenyl-4,5,6,7-tetrahydro-2H-indazole [17].

Yield 98%; white solid; mp 94–96; <sup>1</sup>H NMR (400 MHz,  $CDCl_3$ ):  $\delta_H$  = 1.84 (m, 4H), 2.59 (bs, 2H), 2.81 (bs, 2H), 7.22 (m, 6H), 7.32 (m, 3H)

3w. 2-(4-fluorophenyl)-3-phenyl-4,5,6,7-tetrahydro-2H-indazole.

Yield 90%; brown crystal; mp 84–86°C; IR (KBr,  $cm^{-1}$ ): 3050, 2940, 1517, 1363, 1210, 1166, 964, 845, 741, 588; <sup>1</sup>H NMR (400 MHz,  $CDCl_3$ ):  $\delta_H$  = 1.77 (m, 2H), 1.91 (m, 2H), 2.64 (t,  $J$  = 6.0 Hz, 2H), 2.85 (t,  $J$  = 6.0 Hz, 2H), 7.20 (m, 2H), 7.25 (d,  $J$  = 7.6, 2H), 7.37 (m, 2H), 7.42 (m, 2H); <sup>13</sup>C NMR (100 MHz,  $CDCl_3$ ):  $\delta_C$  = 21.4 (CH<sub>2</sub>), 23.3 (CH<sub>2</sub>), 23.5 (2 x CH<sub>2</sub>), 115.5 (CH), 115.7 (CH), 116.8 (C), 126.4 (CH), 126.5 (CH), 127.8 (CH), 128.4 (2 x CH), 129.2 (2 x CH), 130.6 (C), 136.6 (C), 138.5 (C), 150.4 (C), 161.1 (C).

3x. 2-(2,4-difluorophenyl)-3-phenyl-4,5,6,7-tetrahydro-2H-indazole [22,26].

Yield 47%; brown solid; mp 124–126; <sup>1</sup>H NMR (400 MHz,  $CDCl_3$ ):  $\delta_H$  = 1.85 (m, 4H), 2.62 (t,  $J$  = 6.0 Hz, 2H), 2.79 (t,  $J$  = 6.0 Hz, 2H), 6.80 (m, 2H), 7.14 (dd,  $J$  = 7.0, 2.7 Hz, 2H), 7.27 (m, 3H), 7.39 (m, 1H); <sup>13</sup>C NMR (100 MHz,  $CDCl_3$ ):  $\delta_C$  = 21.5 (CH<sub>2</sub>), 23.2 (CH<sub>2</sub>), 23.4 (CH<sub>2</sub>), 23.5 (CH<sub>2</sub>), 104.8 (CH,  $J_{C-F}$  = 25 Hz), 111.8 (CH,  $J_{C-F}$  = 25 Hz), 115.9 (C), 125.1 (C,  $J_{C-F}$  = 24.0 Hz), 127.9 (CH), 128.4 (4 x CH), 129.8 (CH,  $J_{C-F}$  = 20.0 Hz), 140.3 (C), 151.1 (C), 154.4 (C,  $J_{C-F}$  = 21.0 Hz), 159.4 (C,  $J_{C-F}$  = 24.0 Hz), 164.5 (C,  $J_{C-F}$  = 21.0 Hz); HRMS (ESI, m/z): Calcd for  $C_{19}H_{17}F_2N_2$  [M+H]<sup>+</sup> 311.1360 found 311.1335.

3y. 2-(naphthalen-1-yl)-3-phenyl-4,5,6,7-tetrahydro-2H-indazole.

Yield 47%; brown solid; mp, IR (KBr,  $cm^{-1}$ ): <sup>1</sup>H NMR (400 MHz,  $CDCl_3$ ):  $\delta_H$  = 1.97–2.06 (m, 4H), 2.82 (s, 2H), 2.97 (t,  $J$  = 6.2 Hz, 2H), 7.16–7.23 (m, 5H), 7.33–7.36 (m, 1H), 7.45 (t,  $J$  = 8.0 Hz, 1H), 7.54–7.58 (m, 2H), 7.83–7.86 (m, 1H), 7.91–7.97 (m, 2H); <sup>13</sup>C NMR (100 MHz,  $CDCl_3$ ):  $\delta_C$  = 21.8 (CH<sub>2</sub>), 23.3 (CH<sub>2</sub>), 23.6 (2 x CH<sub>2</sub>), 115.3 (C), 123.7 (CH), 124.9 (CH), 125.5 (CH), 126.3 (CH), 126.9 (CH), 127.4 (CH), 127.9 (CH), 128.1 (2 x CH), 128.4 (2 x CH), 128.5 (CH), 130.6 (C), 134.2 (C), 137.0 (C), 140.6 (C), 150.3 (C); HRMS (ESI, m/z): Calcd for  $C_{23}H_{21}N_2$  [M+H]<sup>+</sup> 325.1705 found 325.1729.

3z. 3-methyl-4,5-dihydro-1H-benzog[indazole] [30–33].

Yield 92 %; white solid; mp 143–145; IR (KBr,  $cm^{-1}$ ): 3136, 3057, 2919, 2883, 2827, 2799 1608, 1568, 1508; <sup>1</sup>H NMR (400 MHz, DMSO):  $\delta_H$  = 2.19 (s, 3H), 2.59 (t,  $J$  = 7.3 Hz, 2H), 2.86 (t,  $J$  = 7.3 Hz, 2H), 3.42 (bs, 1H), 7.15 (t,  $J$  = 7.4 Hz, 1H), 7.23 (t,  $J$  = 7.5 Hz, 2H), 7.67 (d,  $J$  = 7.5 Hz, 1H), 12.44 (bs, 1H); HRMS (ESI, m/z): Calcd for  $C_{12}H_{13}N$  [M+H]<sup>+</sup> 185.1079 found 185.1093.

3aa. 1-(4-bromophenyl)-3-methyl-4,5-dihydro-1H-benzog[indazole].

Yield 43%; orange solid; mp 121–123; IR (KBr,  $cm^{-1}$ ): 3037, 2907, 2846, 1679, 1605, 1496, 1066; <sup>1</sup>H NMR (400 MHz, DMSO-*d*<sub>6</sub>):  $\delta_H$  = 2.19 (s, 3H), 2.58 (t,  $J$  = 7.3 Hz, 2H), 2.91 (t,  $J$  = 7.3 Hz, 2H), 6.74 (d,  $J$  = 7.5 Hz, 1H), 7.05 (t,  $J$  = 7.5 Hz, 1H), 7.15 (t,  $J$  = 7.3 Hz, 1H), 7.33 (d,  $J$  = 7.3 Hz, 1H), 7.38 (d,  $J$  = 8.0 Hz, 2H), 7.68 (d,  $J$  = 8.0 Hz, 2H); <sup>13</sup>C NMR (100 MHz, DMSO-*d*<sub>6</sub>):  $\delta_C$  = 11.1 (CH<sub>3</sub>), 18.2 (CH<sub>2</sub>), 29.5 (CH<sub>2</sub>), 118.5 (C), 120.1 (C), 121.9 (CH), 126.0 (C), 126.1 (CH), 126.7 (2 x CH), 127.1 (CH), 128.4 (CH), 131.9 (2 x CH), 136.5 (C), 137.1 (C), 139.4 (C), 145.5 (C).

3ab. 4-(3-methyl-4,5-dihydro-1H-benzog[indazole]-1-yl)benzoic acid.

Yield 43%; orange solid; mp 258–260; IR (KBr,  $cm^{-1}$ ): 3453, 3214, 2935, 2891, 2835, 2640, 1701, 1646, 1607; <sup>1</sup>H NMR (400 MHz, DMSO-*d*<sub>6</sub>):  $\delta_H$  = 2.21 (s, 3H), 2.59 (t,  $J$  = 7.3 Hz, 2H), 2.93 (t,  $J$  = 7.3 Hz, 2H), 6.77 (d,  $J$  = 7.5 Hz, 1H), 7.05 (t,  $J$  = 7.4 Hz, 1H), 7.17 (t,  $J$  = 7.3 Hz, 1H), 7.35 (d,  $J$  = 7.5 Hz, 1H), 7.55 (d,  $J$  = 8.0 Hz, 2H), 8.04 (d,  $J$  = 8.0 Hz, 2H), 12.07 (bs, 1H); <sup>13</sup>C NMR (100 MHz, DMSO-*d*<sub>6</sub>):  $\delta_C$  = 11.5 (CH<sub>3</sub>), 18.7 (CH<sub>2</sub>), 29.9 (CH<sub>2</sub>), 119.7 (C), 122.6 (CH), 124.7 (2 x CH), 126.5 (CH), 127.6 (CH), 128.8 (CH), 129.7 (C), 130.6 (2 x CH), 137.0 (C), 137.6 (C), 143.8 (C), 146.4 (C), 166.8 (C), 201.2 (C); HRMS (ESI, m/z): Calcd for  $C_{19}H_{17}N_2O_2$  [M+H]<sup>+</sup> 305.1290 found 305.1275

3ac. 1-(4-chlorophenyl)-3-methyl-4,5-dihydro-1H-benzog[indazole].

Yield 65%; yellow solid; mp 139–141; IR (KBr,  $cm^{-1}$ ): 3040, 2957, 2921, 2846 1600, 1543, 1498, 1089; <sup>1</sup>H NMR (400 MHz, DMSO-*d*<sub>6</sub>):  $\delta_H$  = 2.19 (s, 3H), 2.59 (t,  $J$  = 7.3 Hz, 2H), 2.93 (t,  $J$  = 7.3 Hz, 2H), 6.73 (d,  $J$  = 7.7 Hz, 1H), 7.06 (t,  $J$  = 7.7 Hz, 1H), 7.16 (t,  $J$  = 7.5 Hz, 1H), 7.34 (d,  $J$  = 7.5 Hz, 1H), 7.45 (d,  $J$  = 8.0 Hz, 2H), 7.56 (d,  $J$  = 8.0 Hz, 2H); <sup>13</sup>C NMR (100 MHz, DMSO-*d*<sub>6</sub>):  $\delta_C$  = 11.3 (CH<sub>3</sub>), 18.5 (CH<sub>2</sub>), 29.7 (CH<sub>2</sub>), 118.7 (C), 122.1 (CH), 126.3 (CH), 126.8 (CH), 127.4 (2 x CH), 128.7 (CH), 129.2 (2 x CH), 132.1 (C), 136.8 (C), 137.4 (C), 139.3 (C), 145.7 (C).

### 2.3. Molecular docking and ADME prediction

Molecular docking studies were performed using Glide[34] from the suite Maestro (Schrödinger). Glide find the best possible ligand binding pose in a protein grid space, evaluating the energy interactions between [35]. To generate the minimized energy 3D structures *LigPrep* [34,36] module was used under the OPLS-AA force field [37]. The atomic coordinates for protein were extracted from the X-ray crystal structure of BuChE (PDB ID: 4BDS) [38]. The protein was prepared for docking using Protein Preparation Wizard module [36]. Waters molecules were not considered. The center of the grid box was situated using the location of co-crystallized original ligands and was refined and set up as 20 Å. Ligands were docked using the extra precision (XP) mode [39]. The retained best poses were determined by Glide score, visually inspected and the interactions with binding residues were analyzed.

The absorption, distribution, metabolism, excretion properties of the compounds were predicted using *QikProp* [35,40] software from suite Maestro through the calculations processed in normal mode of different descriptors such as octanol/water partitioning coefficient (Log P), surface areas of polar nitrogen and oxygen atoms (PSA), aqueous solubility (Log S), among others. The acceptability of the compounds based on Lipinski's rule [41] was also evaluated.

### 2.4. Cholinergic assay

The evaluation of enzyme inhibition was carried out applying the Ellman's spectrophotometric method [42]. AChE (from *Electrophorus electricus*) and BuChE (from equine serum), 5,5'-dithio-bis-(2-nitrobenzoic acid (DTNB), acetylthiocholine and butyrylthiocholine iodides were purchased from Sigma-Aldrich. The stock solutions of the test compounds were prepared in 100 µL of DMSO and 900 µL of phosphate buffer (8 mmol/L K<sub>2</sub>HPO<sub>4</sub>, 2.3 mmol/L NaH<sub>2</sub>PO<sub>4</sub>, 150 mmol/L NaCl, and 0.05% Tween 20 at pH 7.6). In a 96-well plate, 50 µL of stock solutions were diluted with phosphate buffer to obtain concentrations between 15 – 500 µg/mL for each compound. Enzyme solutions were prepared with a buffer to give 0.25 units/mL and 50 µL was added to the plate. After 30 min of incubation, the substrate solution consistent of Na<sub>2</sub>HPO<sub>4</sub> (40 mmol/L), acetylthiocholine/butyrylthiocholine (0.24 mmol/L) and 0.2 mmol/L of DTNB) was added. The mixture was incubated for another 5 min and the absorption at 405 nm was determined with Microtiter plate reader (Multiskan EX, Thermo). Each compound concentration was tested in triplicate. The IC<sub>50</sub> values were calculated by means of regression analysis.

### 2.5. DPPH radical scavenging activity

The scavenging activities of the compounds were estimated using DPPH as the free radical model according to the method previously described and adapted [43]. Briefly, an aliquot of 1 mL of the tested compound (10–100 µg/mL) and control (2% DMSO), respectively, were mixed with 2 mL of a methanolic solution of DPPH (0.02 mg/mL). The mixture was shaken vigorously and left to stand at room temperature for 5 min in the absence of light. The mixture was measured spectrophotometrically at 517 nm. The free radical scavenging activity was calculated as the percentage of DPPH decoloration using the following equation:

$$\% \text{scavenging DPPH free radical} = 100 \times (1 - \text{AE}/\text{AD})$$

Where AE, is the absorbance of the solution after adding the extract and AD is the absorbance of the blank DPPH solution. Ascorbic acid was used as reference compounds with IC<sub>50</sub> value of 1.5 µg/mL.

### 2.6. Crystallography

XRD data of 3ac were collected at room temperature using a Bruker Kappa CCD diffractometer. Data collection, data reduction, and cell refinement: Bruker Smart, Saintplus, APEX3 [44]. XRD data of 3w were collected at room temperature using a RIGAKU XTA-LAB P200 diffractometer. Data collection, data reduction, and cell refinement: CrystalClear 2.1 [45]. Program used to refine the crystal structures and prepare materials for publication: SHELXL [46], Olex2 [47] and PLATON [48]. The structures were solved by direct methods and refined with the full-matrix least-squares method on F<sup>2</sup>. All H-atoms were positioned geometrically and constrained to ride on their parent atoms.

The structures of 3w and 3ac were further confirmed by SXRD analysis (Fig. 2-ORTEP diagram). The summary of crystallographic data is given in Table 1. The torsion angle of N1-N2-C1-C6 is 132.24(12)° and 116.50(1)° in 3w and 3ac, respectively. This six-membered ring takes a near-enveloped conformation. The Cremer and Pople puckering parameters of the 6-membered ring (C14-C18) in 3w are Q1 = 0.4887(19) Å, θ = 50.9 (2)° and φ = 210.8 (3)° [50]. The Cremer and Pople puckering parameters of the 6-membered ring (C7/C8/C13-C16) in 3ac are Q1 = 0.412(2) Å, θ = 113.7 (3)° and φ = 19.6 (3)° [50]. The six-membered ring adopts a Half-Chair conformation. N1-N2 bonds ranging from 1.367(2) to 1.3637(17) Å in 3w and 3ac. All relevant structural parameters (bond distances and angles) are as expected and in accordance with other organic molecules [51]. Crystallographic data reported in this paper for 3w and 3ac compounds have been uploaded at the Cambridge Crystallographic Data Center (CCDC), No. 1894737 and 1894736, respectively. Copies of the data can be obtained, free of charge, on application to CCDC 12 Union Road, Cambridge CB2 1EZ, UK (Fax: +44-1223-336033 or e-mail: deposit@ccdc.cam.ac.uk).

### 2.7. Quantum chemical calculation: stereo-electronic effect analysis

The theoretical study was realized based on Molecular Quantum Similarity Measure (MQSM), density functions, analyzing a series of reactive descriptors, and Fukui functions. All the structures included in this study were optimized at M02X/6–31G(d, p) level of theory by using the Gaussian 09 package [49]. Details and basis of the methods used are included in the supplementary material.

## 3. Results and discussions

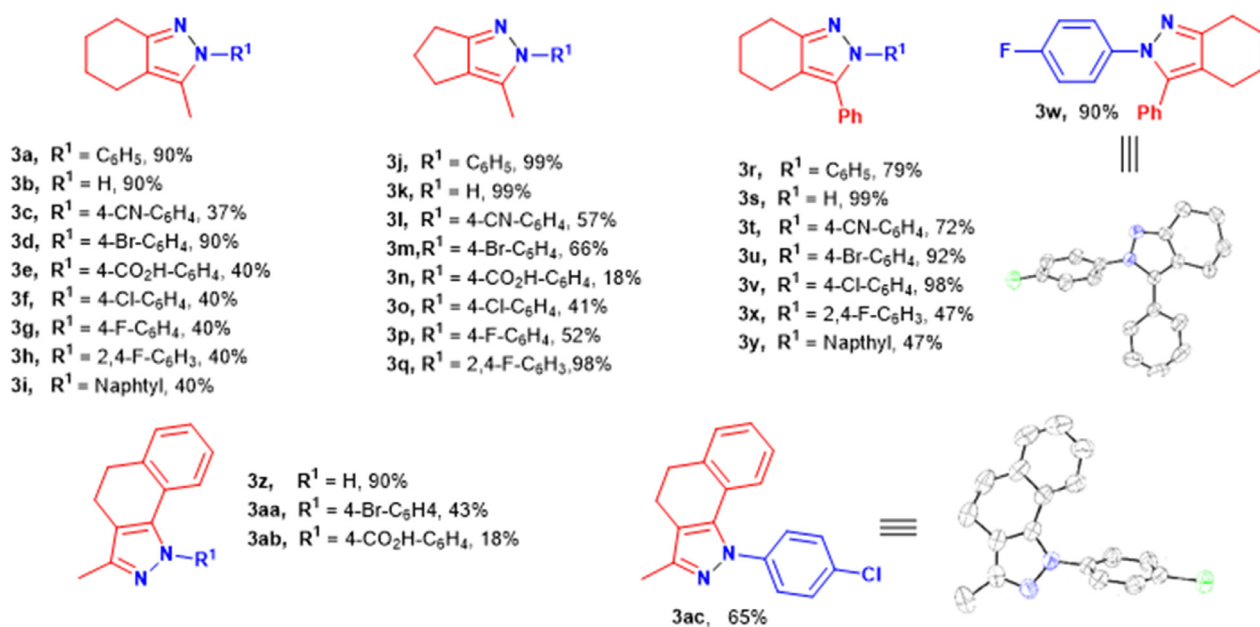
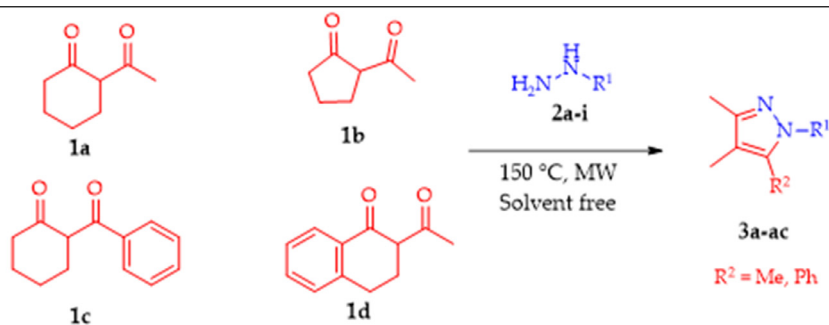
### 3.1. Chemical synthesis

The cyclocondensation of 1,3-dicarbonyl and their equivalent 1,3-dienophilic synthons such as propargylic ketones compounds with hydrazine derivatives represent one of the simplest and most general approaches to the synthesis of pyrazoles and tetrahydroindazoles. When the asymmetric 1,3-dicarbonyl was used the regioselectivity is not favored, the regioisomers aren't distinguishable on TLC (Thin Layer Chromatography) nor separable by column chromatography and had to be detected by <sup>1</sup>H NMR and HPLC analysis. In this work, we offer a convenient highly regioselective synthesis of azoles (pyrazole and indazole) under the microwave (MW) as the energy source (150°C, 10 min). This protocol has the advantages of simple operation, higher yields, low cost, and is an environmentally friendly procedure. Scheme 1 shows the compounds synthesized. These were classified into 4 series according to the common precursor: Series 1 obtained from precursor 1a (3a-3i), series 2 from reagent 1b (3j-3q), series 3 synthesized from 1c (3r-3y) and series 4 formed from 1d (3z - 3ac).

This protocol carried out us to N2-isomers, the N1-isomers were not observed in any of the cases, the regioselectivity of this

**Table 1**  
Crystal data and details of the structure determinations 3w and 3ac

Compound	C <sub>19</sub> H <sub>17</sub> N <sub>2</sub> F (3w)	C <sub>18</sub> H <sub>15</sub> N <sub>2</sub> Cl (3ac)
Crystal shape, color	Polyhedron, colorless	Polyhedron, colorless
Crystal size (mm)	0.40 × 0.20 × 0.08	0.15 × 0.14 × 0.08
Crystal system, Space group	Orthorhombic, Pbc <sub>a</sub>	Monoclinic, P2 <sub>1</sub> /c
a (Å)	17.4515(13)	8.4256(16)
b (Å)	16.5252(12)	20.063(4)
c (Å)	10.3189(7)	9.2168(18)
α (°)	90.0	90.0
β (°)	90.0	102.374(3)
γ (°)	90.0	90.0
V (Å <sup>3</sup> )	2975.9(4)	1521.9(5)
Z	8	4
Wavelength, Mo Kα (Å)	0.71073	0.71073
T (K)	298 (2)	298 (2)
F(000)	1232	616
θ-range (°)	3.16 < θ < 25.2	2.03 < θ < 26.5
hkl-range	-17:22, -21:20, -10:13	-10:10, -25:25, -11:11
μ (mm <sup>-1</sup> )	0.086	0.245
Reflections collected/R <sub>int</sub> /R <sub>σ</sub>	15262/0.041/0.030	12240/0.040/0.042
Reflections unique/ parameters	2206/ 199	1983/ 191
R <sub>1</sub> , wR <sub>2</sub> [F <sup>2</sup> > 2σ (F <sup>2</sup> )]	0.0435, 0.1346	0.0423, 0.1147
Goodness-of-Fit on F <sup>2</sup> (GooF = S)	1.029	0.905
Δρ <sub>max</sub> /Δρ <sub>min</sub> (e Å <sup>-3</sup> )	0.263/-0.427	0.326/-0.217

**Scheme 1.** Synthesized pyrazoles and tetrahydroindazoles.

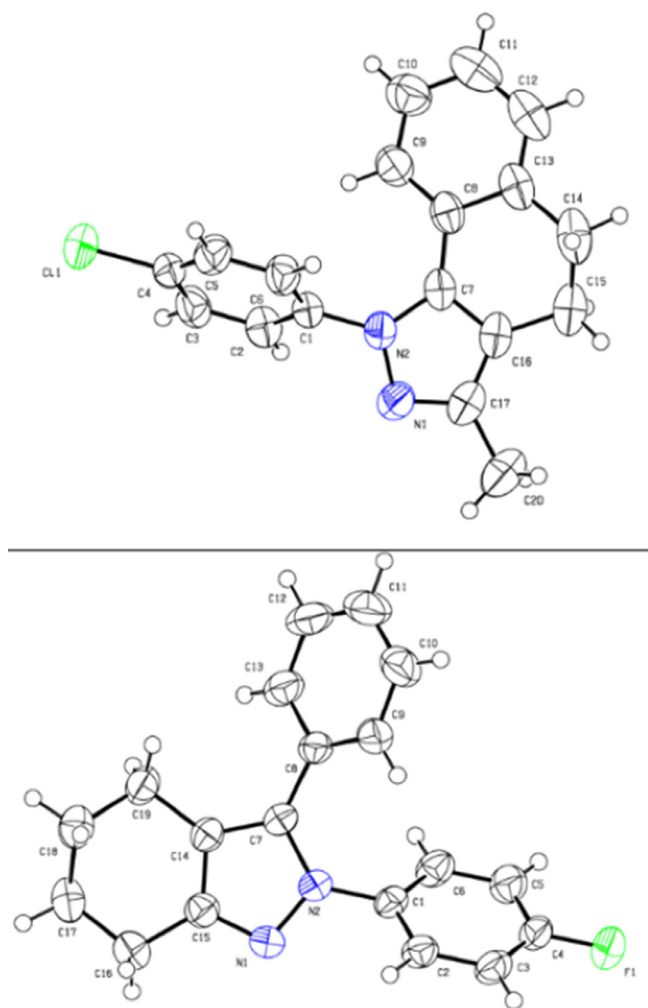


Fig. 2. ORTEP diagram for compounds 3ac (upper) and 3w (lower).

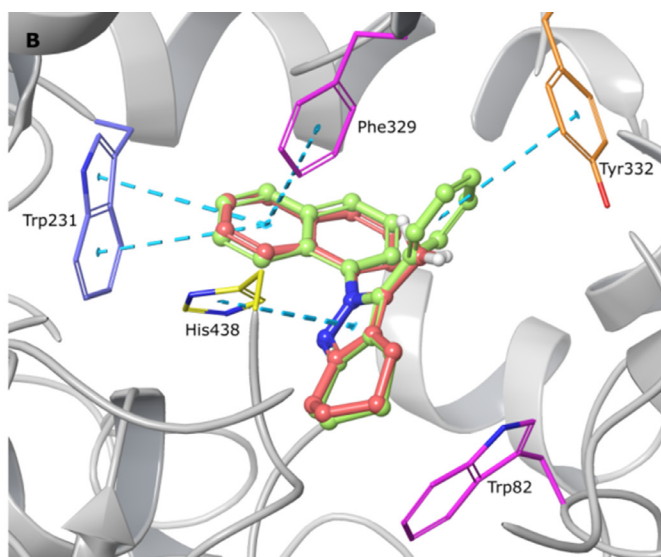
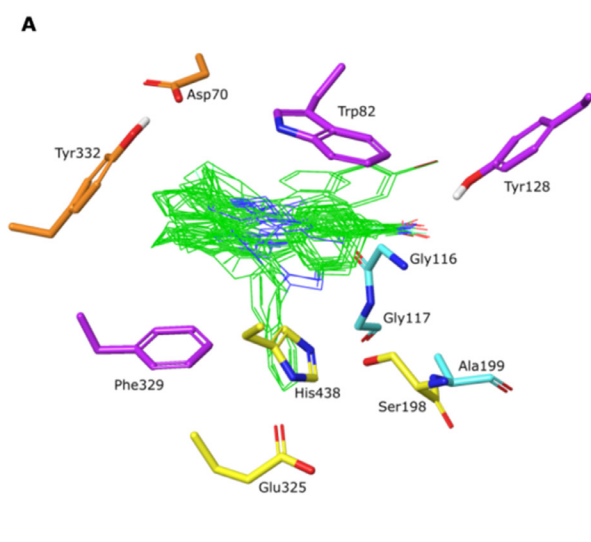


Fig. 3. Predicted binding conformations of new ligands in BuChE active site. The clusters are shown inline representation (green). Residues of BuChE are shown in stick representation. Catalytic triad (yellow), peripheral anionic (orange), anionic site (magenta), oxyanion hole (cyan). B) Binding molecular interactions for compounds 3i (faded red-orange) and 3y (faded yellow-green) within the BuChE binding site. Cyan dotted lines represent  $\pi$ - $\pi$  stacking. Relevant amino acids are shown in a thin tube. Compounds are shown in ball-and-stick representation. The secondary protein structure is depicted as white ribbons.

synthesis was corroborated through single-crystal X-ray diffractions (SXRD) analysis by structure-determination of 3w and 3ac molecules. Steric hindrance can be acclaimed for all asymmetric 1,3-diones to explain the influence on the regioselectivity (This fact, was studied using the energy stabilization on the active conformation). However, the diones 1c and 1d are an exception, since the conjugative effect of the aromatic ring that stabilizes the enol-tautomer, can contribute to increasing the regioselectivity of this process towards the formation of N2-isomer.

### 3.2. AChE and BuChE inhibition assay

The compounds were evaluated against AChE and BuChE enzymes to determine their potential inhibitory capacity. (Table 2). Our results indicated that BuChE was significantly inhibited by the indazole derivatives (3a – 3ac).

Table 2 shows that all compounds tested were selective for BuChE, this selectivity is probably due to some structural differences in the active site of the two enzymes, where the presence of hydrophobic residues in BuChE active site stand out than in AChE they are aromatic. Similarly, it is likely that by having different physiological functions, BuChE has the ability to accept a structural variety of ligands compared to AChE [52]. Likewise, it is observed that the most active compounds 3i and 3y are the only ones with a naphthyl ring as a substitute, which could indicate that this ring has a key role in the selectivity on BuChE.

### 3.3. Molecular docking analysis

To get insight into the intermolecular interactions, a molecular docking study was carried out for the most active and selective compounds against BuChE reported in this work. Molecular docking simulations were performed through software Glide. This software uses a series of hierarchical filters that include a systematic searching approach, sampling the positional, conformational, and orientation space of the ligand [35]. In Fig. 3A is observed that the compounds adopted the same position within the active site. The pyrazole ring was located at the anionic site near the bottom of the active site, which is composed of the amino acids Trp82, Tyr128, and Phe329 (magenta in Fig. 3), (thus) occupying similar space of

**Table 2**  
Inhibitory activity of new compounds on AChE and BChE.

Compound	Anticholinesterase assay (IC <sub>50</sub> )	Compound	Anticholinesterase assay (IC <sub>50</sub> )
	AChE (μM) <sup>a</sup>	BuChE (μM) <sup>a</sup>	AChE (μM) <sup>a</sup> BuChE (μM) <sup>a</sup>
3a [14]	603.27 ± 0.04	8.92 ± 0.01	667.86 ± 0.01 434.62 ± 0.08
3b	172.65 ± 0.01	966.15 ± 0.02	3q 569.21 ± 0.03 340.5 ± 0.02
3c	212.54 ± 0.03	226.95 ± 0.06	3r ≥2006.22 91.14 ± 0.01
3d	216.71 ± 0.03	32.40 ± 0.08	3s ≥837.27 87.78 ± 0.04
3e	205.88 ± 0.07	310.61 ± 0.03	3t ≥554.5 ≥554.50
3f	176.26 ± 0.02	32.71 ± 0.09	3u – –
3g	231.97 ± 0.02	9.39 ± 0.01	3v 216.97 ± 0.03 ≥268.78
3h	144.11 ± 0.01	34.19 ± 0.05	3w 627.51 ± 0.04 97.77 ± 0.02
3i	>632.75	3.59 ± 0.02	3x – –
3j	641.98 ± 0.09	40.00 ± 0.01	3y >511.69 1.65 ± 0.06
3k	666.51 ± 0.03	593.11 ± 0.03	3z 782.12 ± 0.04 ≥3804.65
3l	266.17 ± 0.04	≥743.48	3aa 916.73 ± 0.01 1476.21 ± 0.02
3m	≥1803.98	38.54 ± 0.01	3ab 1823.06 ± 0.05 ≥3571.14
3n	398.41 ± 0.02	1345.05 ± 0.07	3ac ≥3701.42 2973.67 ± 0.09
3o	843.54 ± 0.03	257.62 ± 0.07	Galantamine <sup>a</sup> 0.57 ± 0.10 8.80 ± 0.50

<sup>a</sup> IC<sub>50</sub> ± SEM**Table 3**  
Specific BuChE-ligand interactions, and averaged distances, obtained from molecular docking experiments.

	Residues	N	Distance (Å)
H-bond	Tyr128	4	2.03 ± 0.20
	Gly115	2	2.31 ± 0.05
Halogen bond	Tyr128	4	2.71 ± 0.32
	Trp82	22	4.59 ± 0.59
π-stacking	His438	3	4.94 ± 0.06
	Phe329	2	3.56 ± 0.02
	Tyr332	2	4.86 ± 0.02
	Trp231	2	5.02 ± 0.05

N corresponds to number of compounds that interact with a specific residue.

reference compound tacrine [38]. The specific protein-ligand interactions observed in the representative docking poses are summarized in Table 3.

The compounds 3i and 3y are potent BuChE selective inhibitors (3.59 and 1.65 μM respectively) and present better activity than galantamine, used as a reference control. Fig. 3B shows the interactions of both compounds with different residues of BuChE, mainly π-π stacking (in T-shaped conformation) with some key residues in the binding site. Naphthalene moiety showed a strong contact with Phe329 and Trp231 (from the acyl binding-pocket), while 3y showed an extra hydrophobic interaction with the aromatic residue Tyr332 to 4.85 Å. These interactions allowed pyrazole moiety to stabilize through a π-π stacking with catalytic residue His438.

Likewise, compounds 3a and 3g showed good inhibitory activity and high selectivity against BuChE. They presented a π-π stacking between pyrazole moiety and amino acid residue Trp82 in the mid gorge (not shown). The binding affinity energies of the compound most active show a direct tendency in relation to inhibitory activity (Table 4).

To estimate if the synthesized compounds can be possible candidate drugs for human consumption, the absorption, distribution,

metabolism, and excretion (ADME) of each compound were determined through *in silico* analysis of some pharmaceutical properties and significant physical descriptors as lipophilicity expressed as the octanol/water partition coefficient, aqueous solubility, and hydrogen bond acceptor-donor. Table 5 shows an analysis of the four most active compounds against BuChE. The studied descriptors were found within acceptable rank; thus, there are not any major infraction of the Lipinski's rules [41] with some exceptions (Supplementary Table S1). Other parameters as water solubility (Log S) and PSA, important descriptors in the analysis of membrane penetration, showed values within acceptable range define to human use [53]. In general, the analysis suggested the compounds can be proposed as candidate drugs for BuChE inhibition.

### 3.4. Antioxidant assay

The oxidative stress is associated with an unbalance of reactive oxygen or nitrogen species with the low capacity of endogenous systems to fight against the production of free radicals, which induce damage on biomolecules. This phenomenon is linked to a great number of pathologies, among which the following stand out cancer, neurodegenerative diseases, cardiovascular diseases, and inflammatory diseases, among others [54]. For this reason, the most selective compounds on BuChE were submitted to a free radical trap analysis to identify their potential antioxidant activity (Table 6).

In the results of Table 6, we can see that most compounds have the capacity to trap free-radicals. These can make a synergistic contribution to the possible treatment of AD.

### 3.5. Quantum chemical calculation: stereo-electronic effect analysis

In line with current trends in Computer-Aided Drug Design Quantum Mechanics / Molecular Mechanics (QM / MM) methodologies. In this study, the quantum similarity field is used with the intention of knowing the structural and electronic effects in each series analyzed. Quantum similarity studies allow us to identify

**Table 4**  
Molecular docking results of most active compounds against BuChE.

Compound	XP Glide Score (Kcal/mol)	Interaction type of residue
3a	-5.044	Hydrophobic interaction: Trp82
3g	-5.465	Hydrophobic interaction: Trp82
3i	-7.419	Hydrophobic interaction: Phe329, His438, Trp321
3y	-9.087	Hydrophobic interaction: Phe329, His438, Trp321, Tyr332

**Table 5**  
Physicochemical descriptors calculated for the most active compounds.

Entry	MW (g/mol)	Log P (o/w) <sup>a</sup>	Log S <sup>b</sup>	Donor HB <sup>c</sup>	Acpt HB <sup>d</sup>	PSA <sup>e</sup>	Rule of five
3a	212.294	3.984	4.656	0.000	1.000	16.205	0
3g	230.284	4.308	5.035	0.000	1.000	16.199	0
3i	262.354	4.980	5.739	0.000	1.000	13.582	0
3y	324.424	6.210	7.074	0.000	1.000	14.736	1

<sup>a</sup> log P for octanol/water (-2.0 - -6.5)<sup>b</sup> Predicted aqueous solubility, log S, S in mol dm<sup>-3</sup>(-6.5 - 0.5)<sup>c</sup> Estimated number of H-bonds that would be donated by the solute to water molecules in an aqueous solution<sup>d</sup> Estimated number of H-bonds that would be accepted by solute from water molecules in an aqueous solution<sup>e</sup> Van der Waals surface areas of polar nitrogen and oxygen atoms**Table 6**  
Antioxidant activity results for the most active compounds, DPPH.

Entry	DPPH assay EC <sub>50</sub> (μg/mL) <sup>a</sup>	r <sup>2</sup>
3d	136.049 ± 2.3	0.9282
3e	31.542 ± 1.9	0.9929
3f	188.108 ± 3.1	0.9925
3g	38.404 ± 2.2	0.9741
3h	40.019 ± 1.8	0.9999
3i	46.1391 ± 3.4	0.9595
3j	127.146 ± 2.5	0.9741
3n	42.929 ± 3.7	0.9612
3y	130.413 ± 2.0	0.9654
Ascorbic acid <sup>b</sup>	1.5 ± 0.2	0.9753

<sup>a</sup> EC<sub>50</sub> value: The effective concentration at which the antioxidant activity was 50 %; DPPH. EC<sub>50</sub> values were obtained by interpolation from a linear regression analysis. Values were the mean of three replicates ± SE. r<sup>2</sup> is a statistical measure of how close the data are to the fitted regression line; it is also known as the coefficient of determination or the coefficient of multiple determinations for multiple regressions.<sup>b</sup> Reference compound.

the relationship between biological-activity and stereo-electronic effects in the molecular set, taking as reference the most common structure in the alignment process. In Table 7 it can see that the structural similarity value between 3b and 3a is lower than the

value between 3a and 3i (series 1), this is logical since 3a has a phenyl substituent and 3i a naphthyl group compared to 3b which has a hydrogen atom at the R<sup>1</sup> position. As far as the values of electronic similarity a considerable difference can also be seen between 3b and 3i. These values support the inhibitory behavior of these three compounds, that is, the presence of the phenyl group (3a) improved the inhibitory activity compared to 3b, while the presence of the naphthyl group increased more the enzymatic inhibition. This indicates that aromatic interactions are relevant to the activity and selectivity experimentally observed. In these tables, it is also observed that the presence of withdrawing electron groups on phenyl decreases the biological activity (3e and 3c). This is probably due to the fact that by resonance the electronic aromatic cloud is not constantly available to interact within the active site.

Similarly, when observing the structural similarity values of compounds 3s, 3r and 3y (series 3), the same pattern of series 1 stands out, since the substitution of hydrogen (3s) by phenyl (3r), as well as hydrogen by naphthyl (3y), denotes a marked difference that is expressed in the *in vitro* inhibitory activity. The same behavior can be deduced by observing the values of electronic similarity (Table 8). The presence of withdrawing electron groups on 3t significantly decreases inhibitory activity, which is supported by structural and electronic similarity values between 3t and 3y. This indicates that these compounds are different in both aspects.

**Table 7**  
Matrix of index the similarity quantum of Carbo for the Coulomb and overlap descriptors for series 1

C_Hab	3a	3b	3c	3d	3e	3f	3g	3h	3i*
3a	1.0000								
	1.0000								
3b	0.9173	1.0000							
	0.7434	1.0000							
3c	0.9888	0.8902	1.0000						
	0.9435	0.7014	1.0000						
3d	0.9945	0.8990	0.9983	1.0000					
	0.9777	0.7294	0.9762	1.0000					
3e	0.9678	0.8577	0.9890	0.9866	1.0000				
	0.8524	0.6345	0.8793	0.9015	1.0000				
3f	0.9943	0.8974	0.9980	0.9998	0.9862	1.0000			
	0.9758	0.7242	0.9755	0.9967	0.8968	1.0000			
3g	0.9905	0.8904	0.9945	0.9959	0.9821	0.9972	1.0000		
	0.9175	0.6601	0.9185	0.9216	0.8331	0.9376	1.0000		
3h	0.9828	0.8733	0.9864	0.9880	0.9741	0.9892	0.9915	1.0000	
	0.8497	0.6003	0.8410	0.8486	0.7631	0.8644	0.9197	1.0000	
3i*	0.9606	0.8722	0.9540	0.9607	0.9395	0.9606	0.9568	0.9570	1.0000
	0.7434	0.7530	0.7006	0.7309	0.6329	0.7307	0.6851	0.6448	1.0000

The similarity values were obtained using equation 17 (supporting information) in the Carbo index (equation 2), the Coulomb operator (upper values), and the overlap operator (lower values). Note: The Carbo index is determined in the range of 0 to 1. Where 1.0000 is the self-similarity. \*The most active compound for this series.

**Table 8**

Matrix of index the similarity quantum of Carbó for the Coulomb and overlap descriptors for series 3

C_Hab	3r	3s	3t	3u	3v	3w	3x	3y*
3r	1.0000							
	1.0000							
3s	0.9238	1.0000						
	0.7037	1.0000						
3t	0.9307	0.9987	1.0000					
	0.7344	0.9779	1.0000					
3u	0.9311	0.9976	0.9992	1.0000				
	0.7510	0.9609	0.9839	1.0000				
3v	0.9260	0.9948	0.9963	0.9980	1.0000			
	0.7022	0.9099	0.9181	0.9476	1.0000			
3w	0.9138	0.9868	0.9885	0.9909	0.9930	1.0000		
	0.6750	0.8177	0.8285	0.8627	0.9129	1.0000		
3x	0.9014	0.8349	0.8407	0.8396	0.8343	0.8243	1.0000	
	0.7190	0.5743	0.5928	0.5892	0.5450	0.5016	1.0000	
3y*	0.8428	0.8199	0.8763	0.8231	0.8172	0.8181	0.9293	1.0000
	0.6064	0.4855	0.4750	0.5004	0.4647	0.4376	0.8294	1.0000

The similarity values were obtained using equation 17 (supporting information) in the Carbó index (equation 2), the Coulomb operator (upper values), and the overlap operator (lower values).

Note: The Carbó index is determined in the range of 0 to 1. Where 1.0000 is the self-similarity.

\*The most active compound for this series.

On the other hand, the value of structural similarity between 3i and 3y is low, which is logical since these compounds come from different 1,3-diketones precursors. Thus, while 3i has a methyl group on its scaffold, 3y has a phenyl substituent. Interestingly, these two compounds have a fairly high electronic similarity value (comparing 3y with compounds from all series). This would explain why 3i and 3y were the compounds with the highest selective and inhibitory capacity in the series. This same pattern is observed when comparing the structural and electronic similarity values of compounds 3b and 3s, where it is evident that the presence of aromatic rings adjacent to the pyrazole ring increases the inhibitory activity and selectivity against BuChE.

In Tables 7 and 8, we can see that all the electronic similarity values are higher compared to the structural similarity values. Therefore, due the electronic effects are most relevant than the structural effects. The reactivity descriptors of the synthesized compounds like chemical potential, hardness, and softness, among others are showed in (Supp. Info Table S2). All compounds have high hardness and low electrophilicity values, which indicate that the nature of the stabilization process in the active site can be a non-covalent process. These outcomes are consistent with the features reported for these compounds [55,56].

#### 4. Conclusion

We are synthesized a set of pyrazoles and tetrahydroindazoles derivatives in mild condition, moderated to good yield. These compounds were characterized by spectroscopy technic (FT-IR, <sup>1</sup>H-NMR, <sup>13</sup>C-NMR) and mass spectrometry. The structural and electronic similarity calculations allowed us to identify and to explain biological activity. The regioselectivity of this synthesis was corroborated through by single-crystal X-ray diffractions analysis. Enzymatic assay showed that compounds synthesized had moderate inhibitory effect against BuChE with the compounds 3i and 3y showing the best results 3.59  $\mu$ M and 1.65  $\mu$ M, respectively. The most active compounds 3i and 3y are the only ones of all the series with naphthyl substitutes, which indicates a possible incidence of this ring in their activity. Both pyrazoles and tetrahydroindazoles derivatives were more selective by BuChE than AChE, the compounds 3i and 3y were almost 170 times and 300 times more selective by BuChE, respectively and these two compounds were more active than drug reference (galantamine) too. The most compounds showed capacity to trap free-radicals through DPPH

method. Molecular docking showed that the orientation of the compounds into active site is uniform, most compound orient de pyrazole ring to catalytic anionic site where interact with residues Trp82, Tyr128, and Phe329 which are reported in literature as important interactions.

#### Declaration of Competing Interest

There are no conflicts to declare.

#### CRediT authorship contribution statement

**Efraín Polo:** Methodology, Investigation, Writing - original draft. **Luis Prent-Peñaloza:** Methodology, Investigation, Writing - original draft. **Yeray A. Rodríguez Núñez:** Methodology, Investigation, Writing - original draft. **Lady Valdés-Salas:** Methodology, Investigation. **Jorge Trilleras:** Conceptualization. **Juan Ramos:** Methodology. **José A. Hena:** Formal analysis. **Antonio Galdámez:** Formal analysis. **Alejandro Morales-Bayuelo:** Software. **Margarita Gutiérrez:** Project administration, Supervision.

#### Acknowledgements

This research was supported by a FONDECYT project number 1150712, Utaica. EP and MG give thanks to the CONICYT scholarship No. 63140046. Y.A.R.N. thanks FONDECYT Post-Doctoral Fellowship No. 3190557.

#### References

- [1] E. Giacobini, Cholinesterase inhibitors: new roles and therapeutic alternatives, *Pharmacol. Res* 50 (2004) 433–440, doi:10.1016/j.phrs.2003.11.017.
- [2] A. Bizzarro, V. Guglielmi, R. Lomastro, A. Valenza, A. Lauria, C. Marra, M.C. Silveri, F.D. Tiziano, C. Brahe, C. Masullo, BuChE K variant is decreased in Alzheimer's disease not in fronto-temporal dementia, *J. Neural Transm* 117 (2010) 377–383, doi:10.1007/s00702-009-0358-y.
- [3] M.M. Goldenberg, Celecoxib, a selective cyclooxygenase-2 inhibitor for the treatment of rheumatoid arthritis and osteoarthritis, *Clin. Ther* 21 (1999) 1497–1513, doi:10.1016/S0149-2918(00)80005-3.
- [4] A.I. Graul, E. Cruces, C. Dulsat, E. Arias, M. Stringer, The Year's New Drugs & Biologics, *Drugs Today* 48 (2012) (2011) 33, doi:10.1358/dot.2012.48.1.1769676.
- [5] R.M. Young, L.M. Staudt, Ibrutinib Treatment of CLL: The Cancer Fights Back, *Cancer Cell* 26 (2014) 11–13, doi:10.1016/j.ccr.2014.06.023.
- [6] J.J. Cui, M. Tran-Dubé, H. Shen, M. Nambu, P.-P. Kung, M. Pairish, L. Jia, J. Meng, L. Funk, I. Botrous, M. McTigue, N. Grodsky, K. Ryan, E. Padrique, G. Alton, S. Timofeevski, S. Yamazaki, Q. Li, H. Zou, J. Christensen, B. Mroczkowski,

- S. Bender, R.S. Kania, M.P. Edwards, Structure Based Drug Design of Crizotinib (PF-02341066), a Potent and Selective Dual Inhibitor of Mesenchymal-Epithelial Transition Factor (c-MET) Kinase and Anaplastic Lymphoma Kinase (ALK), *J. Med. Chem.* 54 (2011) 6342–6363, doi:10.1021/jm2007613.
- [7] L.P.H. Yang, K. McKeage, Axitinib, *Drugs* 72 (2012) 2375–2384, doi:10.2165/11209230-000000000-00000.
- [8] F. Turkan, A. Cetin, P. Taslimi, M. Karaman, İ. Gulçin, Synthesis, biological evaluation and molecular docking of novel pyrazole derivatives as potent carbonic anhydrase and acetylcholinesterase inhibitors, *Bioorganic Chem* 86 (2019) 420–427, doi:10.1016/j.bioorg.2019.02.013.
- [9] A. Kumar, S. Jain, M. Parle, N. Jain, P. Kumar, 3-Aryl-1-phenyl-1H-pyrazole derivatives as new multitarget directed ligands for the treatment of Alzheimer's disease, with acetylcholinesterase and monoamine oxidase inhibitory properties, *EXCLI J* 12 (2013) (2013), doi:10.17877/DE290R-7363.
- [10] E. Khan, Z. Gul, A. Shahzad, M.S. Jan, F. Ullah, M.N. Tahir, A. Noor, Coordination compounds of 4,5,6,7-tetrahydro-1H-indazole with Cu(II), Co(II) and Ag(I): structural, antimicrobial, antioxidant and enzyme inhibition studies, *J. Coord. Chem.* 70 (2017) 4054–4069, doi:10.1080/00958972.2017.1416356.
- [11] D.D. Gaikwad, A.D. Chapolikar, C.G. Devkate, K.D. Warad, A.P. Tayade, R.P. Pawar, A.J. Domb, Synthesis of indazole motifs and their medicinal importance: An overview, *Eur. J. Med. Chem* 90 (2015) 707–731, doi:10.1016/j.ejmech.2014.11.029.
- [12] S.-G. Zhang, C.-G. Liang, W.-H. Zhang, Recent Advances in Indazole-Containing Derivatives: Synthesis and Biological Perspectives, *Molecules* 23 (2018) 2783, doi:10.3390/molecules23112783.
- [13] H. Wang, X. Sun, S. Zhang, G. Liu, C. Wang, L. Zhu, H. Zhang, Efficient Copper-Catalyzed Synthesis of Substituted Pyrazoles at Room Temperature, *Synlett* 29 (2018) 2689–2692, doi:10.1055/s-0037-1610330.
- [14] M. Curini, O. Rosati, V. Campagna, F. Montanari, G. Cravotto, M. Boccalini, Layered Zirconium Sulfophenyl Phosphonate as Heterogeneous Catalyst in the Synthesis of Pyrazoles and 4,5,6,7-Tetrahydro-1(2)H-indazoles, *Synlett* (2005) 2927–2930, doi:10.1055/s-2005-921904.
- [15] E. Polo, J. Trilleras, J. Ramos, A. Galdámez, J. Quiroga, M. Gutierrez, Efficient MW-Assisted Synthesis, Spectroscopic Characterization, X-ray and Antioxidant Properties of Indazole Derivatives, *Molecules* 21 (2016) 903, doi:10.3390/molecules21070903.
- [16] Steven Jerome, Goddard, Anthony David, Wolf, Substituted cycloalkanopyrazoles and their herbicidal use, DE 2701467 A1, 1977.
- [17] J.W. Lyga, R.M. Patera, M.J. Plummer, B.P. Halling, D.A. Yuhas, Synthesis, mechanism of action, and QSAR of herbicidal 3-substituted-2-aryl-4,5,6,7-tetrahydroindazoles, *Pestic. Sci.* 42 (1994) 29–36, doi:10.1002/ps.2780420106.
- [18] J.W. Lyga, R.N. Henrie, G.A. Meier, R.W. Creekmore, R.M. Patera, Through-space hydrogen-fluorine, carbon-fluorine and fluorine-fluorine spin-spin coupling in 2-phenyl-3-alkyl-4,5,6,7-tetrahydroindazoles, *Magn. Reson. Chem.* 31 (1993) 323–328, doi:10.1002/mrc.1260310402.
- [19] M.I. Rodríguez-Franco, I. Dorronsoro, A. Martínez, C. Pérez, A. Badía, J.E. Ban'os, Synthesis of NewN-(4-Pyridyl)-1-aminopyrazoles and Their Muscarinic and Adrenergic Properties, *Arch. Pharm. (Weinheim)* 333 (2000) 118–122, doi:10.1002/(SICI)1521-4184(20005)333:5:118::AID-ARDP118.3.0.CO;2-Q.
- [20] A. Nakhai, J. Bergman, Synthesis of hydrogenated indazole derivatives starting with  $\alpha,\beta$ -unsaturated ketones and hydrazine derivatives, *Tetrahedron* 65 (2009) 2298–2306, doi:10.1016/j.tet.2009.01.041.
- [21] O. Rosati, M. Curini, M.C. Marcotullio, A. Macchiarulo, M. Perfumi, L. Mattioli, F. Rismondo, G. Cravotto, Synthesis, docking studies and anti-inflammatory activity of 4,5,6,7-tetrahydro-2H-indazole derivatives, *Bioorg. Med. Chem.* 15 (2007) 3463–3473, doi:10.1016/j.bmc.2007.03.006.
- [22] K.Y. Lee, J.M. Kim, J.N. Kim, Regioselective synthesis of 1,3,4,5-tetrasubstituted pyrazoles from Baylis-Hillman adducts, *Tetrahedron Lett* 44 (2003) 6737–6740, doi:10.1016/S0040-4039(03)01648-4.
- [23] C.A. Dvorak, D.A. Rudolph, S. Ma, N.I. Carruthers, Palladium-Catalyzed Coupling of Pyrazole Triflates with Arylboronic Acids, *J. Org. Chem.* 70 (2005) 4188–4190, doi:10.1021/jo0477897.
- [24] A.J. Nunn, F.J. Rowell, Synthesis of 3-alkyl-1-aryl-6,7-dihydro-6,6-dimethylindazol-4(5H)-ones, 2,3-diaryl-4,5,6,7-tetrahydroindazoles, and related compounds, *J. Chem. Soc. Perkin 1* (1975) 2435, doi:10.1039/p19750002435.
- [25] Ya.Ya. Ozol, É.É. Liepin'sh, G.Ya. Dubur, Reaction of 2-aryl-1-cyclohexanones and their 6-amino derivatives with hydrazines, *Chem. Heterocycl. Compd.* 11 (1975) 1315–1317, doi:10.1007/BF00474463.
- [26] K.Y. Lee, S. Gowrisankar, J.N. Kim, Facile synthesis of 2H-indazole derivatives starting from the Baylis-Hillman adducts of 2-cyclohexen-1-one, *Tetrahedron Lett* 46 (2005) 5387–5391, doi:10.1016/j.tetlet.2005.05.149.
- [27] V. Lellek, C. Chen, W. Yang, J. Liu, X. Ji, R. Faessler, An Efficient Synthesis of Substituted Pyrazoles from One-Pot Reaction of Ketones, Aldehydes, and Hydrazine Monohydrochloride, *Synlett* 29 (2018) 1071–1075, doi:10.1055/s-0036-1591941.
- [28] R.R. Merchant, D.M. Allwood, D.C. Blakemore, S.V. Ley, Regioselective Preparation of Saturated Spirocyclic and Ring-Expanded Fused Pyrazoles, *J. Org. Chem.* 79 (2014) 8800–8811, doi:10.1021/jo501624t.
- [29] B. Chen, C. Yu, G. Zhang, A Novel Method to Prepare Multisubstituted Pyrazoles, *Chin. J. Org. Chem.* 35 (2015) 625, doi:10.6023/cjoc201501037.
- [30] V. Bertolasi, P. Gilli, V. Ferretti, G. Gilli, C. Fernández-Castaño, Self-assembly of N-H-pyrazoles via intermolecular N–H...N hydrogen bonds, *Acta Crystallogr. B* 55 (1999) 985–993, doi:10.1107/S0108768199004966.
- [31] R.M. Claramunt, C. López, M.A. García, G.S. Denisov, I. Alkorta, J. Elguero, Protonation and phase effects on the NMR chemical shifts of imidazoles and pyrazoles: experimental results and GIAO calculationsElectronic supplementary information (ESI) available: absolute and relative shieldings calculated at the B3LYP/6-311++G\*\*//B3LYP/6-311++G\*\* level for compounds V to XXI as well as pyrazole and 3,5-dimethylpyrazole dimers, trimers and tetramers (420 shieldings), New J. Chem. 27 (2003) 734–742 <http://www.rsc.org/suppdata/nj/b2/b210251j/>, doi:10.1039/b210251j.
- [32] A.L. Rheingold, R.L. Ostrander, B.S. Haggerty, S. Trofimenko, Homoscorpionate (Tris(pyrazolyl)borate) Ligands Containing Tethered 3-Phenyl Groups, *Inorg. Chem.* 33 (1994) 3666–3676, doi:10.1021/ic00095a009.
- [33] C. Lopez, R.Ma. Claramunt, S. Trofimenko, J. Elguero, A <sup>13</sup>C NMR spectroscopy study of the structure of N-H pyrazoles and indazoles, *Can. J. Chem.* 71 (1993) 678–684, doi:10.1139/v93-092.
- [34] R.A. Friesner, J.L. Banks, R.B. Murphy, T.A. Halgren, J.J. Klicic, D.T. Mainz, M.P. Repasky, E.H. Knoll, M. Shelley, J.K. Perry, D.E. Shaw, P. Francis, P.S. Shenkin, Glide: A New Approach for Rapid, Accurate Docking and Scoring. 1. Method and Assessment of Docking Accuracy, *J. Med. Chem.* 47 (2004) 1739–1749, doi:10.1021/jm0306430.
- [35] R.A. Friesner, J.L. Banks, R.B. Murphy, T.A. Halgren, J.J. Klicic, D.T. Mainz, M.P. Repasky, E.H. Knoll, M. Shelley, J.K. Perry, D.E. Shaw, P. Francis, P.S. Shenkin, Glide: A New Approach for Rapid, Accurate Docking and Scoring. 1. Method and Assessment of Docking Accuracy, *J. Med. Chem.* 47 (2004) 1739–1749, doi:10.1021/jm0306430.
- [36] G. Madhavi Sastry, M. Adzhigirey, T. Day, R. Annabhimoju, W. Sherman, Protein and ligand preparation: parameters, protocols, and influence on virtual screening enrichments, *J. Comput. Aided Mol. Des.* 27 (2013) 221–234, doi:10.1007/s10822-013-9644-8.
- [37] W.L. Jorgensen, D.S. Maxwell, J. Tirado-Rives, Development and Testing of the OPLS All-Atom Force Field on Conformational Energetics and Properties of Organic Liquids, *J. Am. Chem. Soc.* 118 (1996) 11225–11236, doi:10.1021/ja9621760.
- [38] F. Nachon, E. Carletti, C. Ronco, M. Trovaslet, Y. Nicolet, L. Jean, P.-Y. Renard, Crystal structures of human cholinesterases in complex with huprine W and tacrine: elements of specificity for anti-Alzheimer's drugs targeting acetyl- and butyryl-cholinesterase, *Biochem. J.* 453 (2013) 393–399, doi:10.1042/BJ20130013.
- [39] R.A. Friesner, R.B. Murphy, M.P. Repasky, L.L. Frye, J.R. Greenwood, T.A. Halgren, P.C. Sanschagrin, D.T. Mainz, Extra Precision Glide, Docking and Scoring Incorporating a Model of Hydrophobic Enclosure for Protein-Ligand Complexes, *J. Med. Chem.* 49 (2006) 6177–6196, doi:10.1021/jm051256o.
- [40] F. Caporuscio, G. Rastelli, C. Imbriano, A. Del Rio, Structure-Based Design of Potent Aromatase Inhibitors by High-Throughput Docking, *J. Med. Chem.* 54 (2011) 4006–4017, doi:10.1021/jm2000689.
- [41] C.A. Lipinski, F. Lombardo, B.W. Dominy, P.J. Feeney, Experimental and computational approaches to estimate solubility and permeability in drug discovery and development settings, *Adv. Drug Deliv. Rev.* 23 (1997) 3–25, doi:10.1016/S0169-409X(96)00423-1.
- [42] G.L. Ellman, K.D. Courtney, V. Andres jr., R.M. Featherstone, A new and rapid colorimetric determination of acetylcholinesterase activity, *Biochem. Pharmacol.* 7 (1961) 88–95, doi:10.1016/0006-2952(61)90145-9.
- [43] W. Brand-Williams, M.E. Cuvelier, C. Berset, Use of a free radical method to evaluate antioxidant activity, *LWT - Food Sci. Technol.* 28 (1995) 25–30, doi:10.1016/S0023-6438(95)80008-5.
- [44] BrukerAPEX3, Bruker ASX Inc., Madison, Wisconsin, USA, 2014 n.d..
- [45] RigakuCrystalClear-SM Expert, Rigaku Corporation, Tokyo, Japan, 2011 n.d..
- [46] G.M. Sheldrick, SHELXT - Integrated space-group and crystal-structure determination, *Acta Crystallogr. Sect. Found. Adv* 71 (2015) 3–8, doi:10.1107/S2053273314026370.
- [47] O.V. Dolomanov, L.J. Bourhis, R.J. Gildea, J.A.K. Howard, H. Puschmann, OLEX2 : a complete structure solution, refinement and analysis program, *J. Appl. Crystallogr* 42 (2009) 339–341, doi:10.1107/S0021889808042726.
- [48] A.L. Spek, Structure validation in chemical crystallography, *Acta Crystallogr. D Biol. Crystallogr.* 65 (2009) 148–155, doi:10.1107/S090744490804362X.
- [49] M. Frisch, G. Trucks, H. Schlegel, G. Scuseria, M. Robb, J. Cheeseman, J. Montgomery, T. Vreven, K. Kudin, J. Burant, J. Millam, S. Iyengar, J. Tomasi, V. Barone, B. Mennucci, M. Cossi, G. Scalmani, N. Rega, G. Petersson, H. Nakatsuji, M. Hada, M. Ehara, K. Toyota, R. Fukuda, J. Hasegawa, M. Ishida, T. Nakajima, Y. Honda, O. Kitao, H. Nakai, M. Klene, X. Li, J. Knox, H. Hratchian, J. Cross, V. Bakken, C. Adamo, J. Jaramillo, R. Gomperts, R. Stratmann, O. Yazyev, A. Austin, R. Cammi, C. Pomelli, J. Ochterski, P. Ayala, K. Morokuma, G. Voth, P. Salvador, J. Dannenberg, V. Zakrzewski, S. Dapprich, A. Daniels, M. Strain, O. Farkas, D. Malick, A. Rabuck, K. Raghavachari, J. Foresman, J. Ortiz, Q. Cui, A. Baboul, S. Clifford, J. Cioslowski, B. Stefanov, G. Liu, A. Liashenko, P. Piskorz, I. Komaromi, R. Martin, D. Fox, T. Keith, A. Laham, C. Peng, A. Nanayakkara, M. Challacombe, P. Gill, B. Johnson, W. Chen, M. Wong, C. Gonzalez, J. Pople, Gaussian 09, Gaussian Inc, Wallingford CT, 2009.
- [50] D. Cremer, J.A. Pople, General definition of ring puckering coordinates, *J. Am. Chem. Soc.* 97 (1975) 1354–1358, doi:10.1021/ja00839a011.
- [51] F.H. Allen, D.G. Watson, L. Brammer, A.G. Orpen, R. Taylor, Typical interatomic distances: organic compounds, in: E. Prince (Ed.), *Int. Tables Crystallogr.*, Ed.1st ed., International Union of Crystallography, Chester, England, 2006, pp. 790–811, doi:10.1107/97809553602060000621.
- [52] Y. Nicolet, O. Lockridge, P. Masson, J.C. Fontecilla-Camps, F. Nachon, Crystal Structure of Human Butyrylcholinesterase and of Its Complexes with Substrate and Products, *J. Biol. Chem.* 278 (2003) 41141–41147, doi:10.1074/jbc.M210241200.

- [53] K.D. Singh, P. Kirubakaran, S. Nagarajan, S. Sakkiah, K. Muthusamy, D. Velmurgan, J. Jeyakanthan, Homology modeling, molecular dynamics, e-pharmacophore mapping and docking study of Chikungunya virus nsP2 protease, *J. Mol. Model.* 18 (2011) 39–51, doi:[10.1007/s00894-011-1018-3](https://doi.org/10.1007/s00894-011-1018-3).
- [54] A.M. Pisoschi, A. Pop, The role of antioxidants in the chemistry of oxidative stress: A review, *Eur. J. Med. Chem.* 97 (2015) 55–74, doi:[10.1016/j.ejmech.2015.04.040](https://doi.org/10.1016/j.ejmech.2015.04.040).
- [55] M. Pohanka, Inhibitors of Acetylcholinesterase and Butyrylcholinesterase Meet Immunity, *Int. J. Mol. Sci* 15 (2014) 9809–9825, doi:[10.3390/ijms15069809](https://doi.org/10.3390/ijms15069809).
- [56] M.A. Kamal, S. Shakil, M.S. Nawaz, Q. Yu, D. Tweedie, Y. Tan, X. Qu, N.H. Greig, Inhibition of Butyrylcholinesterase with Fluorobenzylcysteine, An Experimental Alzheimer's Drug Candidate: Validation of Enzoinformatics Results by Classical and Innovative Enzyme Kinetic Analyses, *CNS Neurol. Disord. - Drug Targets* (2017) 16, doi:[10.2174/1871527316666170207160606](https://doi.org/10.2174/1871527316666170207160606).